PCCP

ROYAL SOCIETY OF CHEMISTRY

PAPER

View Article Online
View Journal | View Issue

Cite this: *Phys. Chem. Chem. Phys.*, 2021, **23**, 10946

Superatomic and adsorption properties of Ni atom doped Au clusters†

Qiman Liu, *[ab] Pei Fan,[a] Yunhu Hu,[a] Fengwu Wang[a] and Longjiu Cheng *[c]

Due to their strong relativistic effects, Au clusters exhibit many unusual geometric structures. Among them, Au_7^-, Au_8 and Au_9^+ have 18 valence electrons satisfying the magic numbers in the jellium model, respectively, but these three non-spherical clusters are not superatoms. In general, a single dopant atom can drastically change the structural and electronic properties of Au clusters. Here, we searched structures of $NiAu_7^-$, $NiAu_8$ and $NiAu_9^+$ clusters using the genetic algorithm program (GA) combined with density functional theory (DFT). It was found that the alloy clusters are all 3D spherical structures. The molecular orbitals and density of states analysis indicate that they have completely filled superatomic shells ($1S^21P^6$), in which the electronic structure of the Ni atom is d^{10}. Then, the electrostatic potential surfaces of the alloy clusters are analyzed, and the calculated results show that the $NiAu_8$ superatom has remarkable σ-holes with positive potential regions. Moreover, these electron-deficient regions can be considered as interaction sites with some electron donors. After a Lewis base CO gas molecule is adsorbed on the Au-based superatom, we found that the C–O bond distance becomes slightly elongated and its stretching frequency presents a significant red-shift. This is due to the fact that 5d electrons of the Au atom of the $NiAu_8$ transfer towards the anti-bond π orbitals of the CO molecule. Hence, this is an effective strategy for finding new types of superatoms and potential catalysts for covalent bond activation.

Received 7th February 2021,
Accepted 15th April 2021

DOI: 10.1039/d1cp00589h

rsc.li/pccp

1. Introduction

Gold clusters have been the focus of widespread research interest for decades in cluster science because of their potential applications in the fields of catalysis, electronic devices, biolabeling, and so on.[1–8] Au clusters exhibit many unique properties due to the significant s–d hybridization of Au atoms in comparison to that of other coin metals.[9–11] Among the interesting properties, including chemical reactivity, exceptional stability, and the ability to manufacture them in a large range of sizes and shapes, their size-to-size structures are fascinating.[3,12–14] In particular, the relativistic effects and metallophilic interactions of Au lead to gold clusters that have unusual geometric structures.[15,16] For example, gold clusters adopt two-dimensional (2D) structures even at relatively large sizes, whereas the corresponding Cu and Ag clusters are three-dimensional (3D).[11,17] In fact, the geometries of small-sized Au clusters have been well located that display planar structures within 13 atoms, while even more exotic structures possibly appeared at medium size, such as the Au_{20} pyramid and icosahedral Au_{32} cages.[18,19] For Au cluster cations and anions, similar 2D-to-3D structural transitions can also be viewed, but the transition sizes are different.[20,21]

A single dopant atom drastically changes the structural and electronic properties of Au clusters.[22,23] Several theoretical and experimental works have been devoted to the influence of doping on the stability patterns of Au clusters, which are based on different numbers of electrons that can be delocalized depending on the electronic configurations of the dopant atoms. Medel and Khanna found that $CrAu_7^+$, $ScAu_6^+$, and $TiAu_5^+$ are magic species that are revealed by photofragmentation experiments, where the Cr, Sc, and Ti atoms delocalize 2, 3, and 4 electrons, respectively.[24] Bouwen *et al.* suggested that the stabilities of Au clusters can be improved by doping transition metal Y atoms.[25] Pyykkö's group suggested that the icosahedral WAu_{12} cluster showed high chemical stability with a large HOMO–LUMO gap (3.0 eV) and is an 18-electron superatom.[26] Recently, Zhao and Park investigated structure evolutions of transition metal-doped gold clusters MAu_{12} (M = 3d–5d) by systematic DFT calculations.[27]

For metal clusters, they are usually described using a jellium model.[28,29] The central content of the model is that the cluster's

[a] *School of Chemical and Materials Engineering, Huainan Normal University, Huainan 232038, P. R. China. E-mail: qimliu@ustc.edu.cn*
[b] *Anhui Province Key Laboratory of Low Temperature Co-fired Materials, Huainan, 232038, P. R. China*
[c] *Department of Chemistry, Anhui Province Key Laboratory of Chemistry for Inorganic/Organic Hybrid Functionalized Materials, Anhui University, Hefei, 230601, P. R. China. E-mail: clj@ustc.edu.cn*

† Electronic supplementary information (ESI) available. See DOI: 10.1039/d1cp00589h

entire nuclei and innermost lone-pair electrons assumed a uniform background potential of positive charge, where valence electrons of the metal cluster can be free-moving and are controlled by the external charge potential. Hence, the whole cluster can be considered as a superatom, and the energy levels of valence-electron orbitals are filled by $1S^21P^6$ $1D^{10}2S^21F^{14}2P^6$ and so on, associated with magic numbers 2, 8, 18, 34, 40 *etc.* The jellium model is very successful in explaining the stabilities of metal clusters with spherical structures.[30–33] There is an well-known example of the icosahedral Al_{13}, where it has 39 valence electrons and needs one extra electron to close the $2P^6$ superatomic shells.[34]

Besides the unusual structural characteristics, gold clusters have become attractive due to their diverse catalytic applications.[35–37] For example, Pei and co-work performed a comprehensive study of the reaction mechanism of styrene-selective oxidation to benzaldehyde and styrene epoxide on gold clusters, and the major focuses of the work are the intrinsic catalytic selectivity and size-dependent activities of gold clusters toward styrene oxidations.[38] Zeng *et al.* observed that there is a superoxo to peroxo chemisorption transition of O_2 on gold clusters at Au_8^- by photoelectron spectroscopy.[39] Au-based bimetallic clusters also show wonderful catalytic performances in the catalytic oxidation reaction of the CO molecule, water gas conversion and fuel cell reactions in the chemical industry.[40–42] Gao *et al.* reported that the $Au_{43}Cu_{12}$ icosahedron has prospectively catalytic activities for CO oxidation and selectivities for styrene oxidation.[40] In fact, alloy clusters have uneven distributions of charge over their geometrical surfaces and result in the formation of complementary Lewis acid and Lewis base sites that can make clusters reactive. Rodríguez-Kessler and Munoz-Castro found that the Pt_6Ag_6 cluster possesses a closed shell superatom structure, and the stable superatom can act as a promising catalytic candidate in the hydrogenation reaction.[43] Recently, Khanna *et al.* demonstrated that the complementary active sites of superatom clusters are not only very active for breaking the O–H bonds of alcohols and H_2O, but can also break stronger covalent bonds.[44]

Among the Au clusters, Au_7^-, Au_8 and Au_9^+ have 8 valence electrons satisfying the magic numbers in the jellium model, respectively, but these three non-spherical clusters are not superatoms.[1,45] In general, the way in which heteroatoms are introduced can greatly change the geometries and electronic properties of Au clusters. Moreover, the electronic structure of the Ni atom in clusters is $3d^{10}$ or $3d^84s^2$, and may not change the delocalized electron number of doped clusters.[46] Therefore, we searched the structures of $NiAu_7^-$, $NiAu_8$ and $NiAu_9^+$ clusters using the genetic algorithm program (GA) combined with density functional theory (DFT). The results show that the three clusters transform into spherical structures and have completely filled superatomic shells ($1S^21P^6$), in which the electronic structures of Ni atoms are indeed d^{10}. Particularly, we reported the adsorbed behavior that can be analyzed from the Au-based superatom upon Lewis base CO molecule adsorption. The major attention is paid to the fact that the Au-based superatoms may serve as potential catalysts for covalent bond activation.

2. Computational details

In this study, the global minimum (GM) and low-lying structures of $NiAu_7^-$, $NiAu_8$ and $NiAu_9^+$ clusters are searched by an unbiased global method of GA algorithm directly using the DFT functional. The strategy has been frequently used to predict geometric structures of alloy clusters.[47,48] The GA algorithm vests in one search heuristic of evolutionary strategies that mimics the natural evolutionary process to generate successful projects for optimization and search problems. Here, there are more than 1000 samplings that are calculated by the DFT methods in the optimization procedure at each component. In GA-DFT procedures, we scan potential energy surfaces of the alloy clusters at the TPSS/Def2-SVP level[49] to save time, and spin multiplicities are set to 1 (even electrons) or 2 (odd electrons). The search strategy can be summarized as follows: (a) generate *npop* structures randomly to form the starting population of GA. Relax each structure in the population by DFT method at the TPSS/Def2-SVP level with a loose convergence criterion. (b) For *kth* iteration, choose two structures from the population randomly and perform crossover operation to generate one child structure. After mutation operation, relax the child structure by the DFT method at the TPSS/Def2-SVP level with a loose convergence criterion. (c) Input the relaxed structure to the structural bank. Update the population based on similarity and energy. After optimizations of the global search, all isomers ordered by energies are reoptimized at the theoretical TPSS/Def2-TZVP level, and spin multiplicities are set to (1, 3, and 5) or (2, 4, and 6) to find the most stable isomers.[50] The vibration frequencies of them are also checked at the same level to verify that they belong to true local minimums of potential energy surfaces. The molecular electrostatic potential $V(r)$ is adopted to analyze charge distributions on the surfaces of the clusters, and it is rigorously defined from ref. 51. Furthermore, all quantum chemistry computations are performed with the GAUSSIAN 09 package.[52] The visualization of the molecular orbitals (MO) is realized using the MOLEKEL 5.4 program.[53]

3. Results and discussion

3.1 The structures and superatomic characters of $NiAu_7^-$, $NiAu_8$ and $NiAu_9^+$ clusters

We have summarized the literature on geometric structures of the small-sized Au clusters, and found that the anion Au_7^- cluster is in C_{2v} symmetry.[1,54] Although the cluster has 8 valence electrons, the planar geometry does not satisfy the spherical superatomic model. In comparison, isoelectronic Cu_7^- and Ag_7^- have spherical structures.[55] Since the Au_7^- cluster satisfies the magic number of the Jellium model, it is possible to transform the current structure into a 3D structure by doping one atom without changing the total numbers of

delocalized electrons of the cluster. Of course, there is a prerequisite to ensure that the doped atom does not contribute excess delocalized electrons to the Au-based cluster.

The 3d electrons of the Ni atom as lone pairs can be completely localized, and donate zero electron to cluster bonding. Such a situation can be seen in some Ni-alloy clusters.[46] Furthermore, we retrieved the relevant literature and did not find that anyone has reported the structure of $NiAu_7^-$ before. Following the above idea, we started to use the GA-DFT program developed by our research group to perform an unbiased global search on the structure of $NiAu_7^-$ clusters. All obtained isomer structures are finally determined at the theoretical level of TPSS/Def2-TZVP. This functional with the basis set has been widely used in many Au cluster systems, and it has been strictly proven to be reliable. Due to the fact that Ni is a magnetic atom, we have considered possible high-spin configurations during the sampling of the structures.

Fig. 1 shows the isomer shapes of the $NiAu_7^-$ cluster and their point group symmetry, and relative energies are arranged in order from low to high. Vibration frequency analyses show that these isomers indeed correspond to real local minimums on the potential energy surfaces. Among $NiAu_7^-$ isomers, the lowest energy is a cap structure with C_{2v} symmetry, and the Ni atom is in the endohedrally high coordination. The electronic state of the C_{2v} structure was singlet. The other isomers are also 3D spherical structures. We reoptimized the isomers of the $NiAu_7^-$ cluster using other density functionals and found that the C_{2v} structure is still a global minimum. In addition, there are geometric configurations with the same structural skeleton but different types of atoms in different positions in the isomers, indicating that the search program we used can handle the HOMOTOP problem in binary clusters well.[56] In comparison, the optimal structure of the ground state of Au_7^- and most of the isomers reported in previous literature belong to the 2D geometries.[54,57] Obviously, the doping of the Ni atom significantly modulates the structure of the pure Au_7^- cluster. Moreover, we found that the embedding energies (EE) of the Ni atom within Au-based clusters are very large,[58] and the details of EE calculations are shown in Table S1 (ESI†). The good news is that regardless of whether the electronic structure of the $NiAu_7^-$ cluster finally conforms to the superatomic model, only judging from the geometric structure is the result we want.

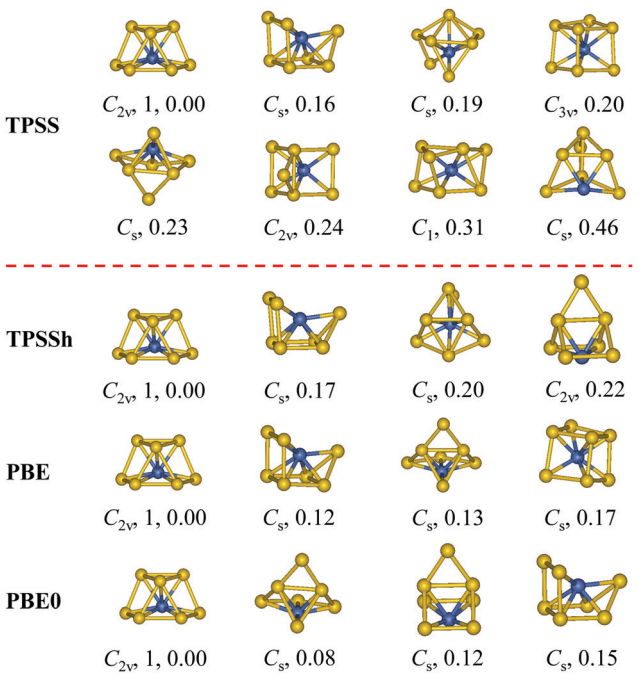

Fig. 1 The low-energy isomers of $NiAu_7^-$ cluster at different density functional levels. Labeled are symmetry, energy (eV) relative to the GM one and spin multiplicities.

Since the geometric structure of the $NiAu_7^-$ cluster conforms to our expectation, does its electronic structure also satisfy the superatomic model? We know that each Au atom has one valence electron, and the Ni atom has 10 valence electrons. So the $NiAu_7^-$ cluster has 18 valence electrons in total. Do these 18 valence electrons really contribute to the Au alloy superatom? Fig. 2a shows the molecular orbitals (MOs) of $NiAu_7$, from which one S-type and three P-type superatomic orbitals can be easily identified. The details of MO diagrams and orbital energies (a.u.) of the $NiAu_7^-$ cluster are given in Fig. S1 (ESI†). Among them, there are five d-type lone pairs that are completely localized on the Ni atom in terms of orbital shapes and energies (HOMO, HOMO−1, HOMO−2, HOMO−3, HOMO−4, HOMO−5). So, it is clear that the eight Au atoms provide eight delocalized electrons required by the $NiAu_7^-$ superatom, while the electrons from the Ni atom do not contribute. To further confirm this result, we also calculated the density of states (TDOS) of the $NiAu_7^-$ superatom. As shown in Fig. 2b, within the energy range of the four superatomic orbitals ($1S^21P^6$), the TDOS of the $NiAu_7^-$ is almost entirely derived from Au atoms, while the contribution of Ni atom at this time is almost negligible, which is exactly consistent with the above MO analysis results.

It has been confirmed that the $NiAu_7^-$ cluster has the 18e superatomic properties, and the calculated results are consistent with our assumptions, indicating that the research idea and calculation method are feasible. Importantly, we found that the electronic structure of the Ni atom in the doped cluster is d^{10}, which indicates that its 10 valence electrons are completely localized. By following the same strategy, more new types of Au-based superatoms can be found. Therefore, we searched the geometric structures of $NiAu_8$ and $NiAu_9^+$ clusters at the same theoretical level, respectively. Fig. 3a shows the isomer shapes of the $NiAu_8$ cluster and their point group symmetry, and relative energies are also arranged in order from low to high.

For the neutral $NiAu_8$, the lowest energy structure of all the searched isomers is also in C_{2v} symmetry, in which the transition metal Ni atom also located at high coordination. The isomers that are nearly degenerate in energy with the ground state structure are 3D spherical. After careful comparison, it is found that $NiAu_8$ and $NiAu_7^-$ have different structural frameworks, though the former structure can be obtained by attaching one Au atom to the latter. Then, we used the same method to calculate the molecular orbitals of $NiAu_8$ after the structure

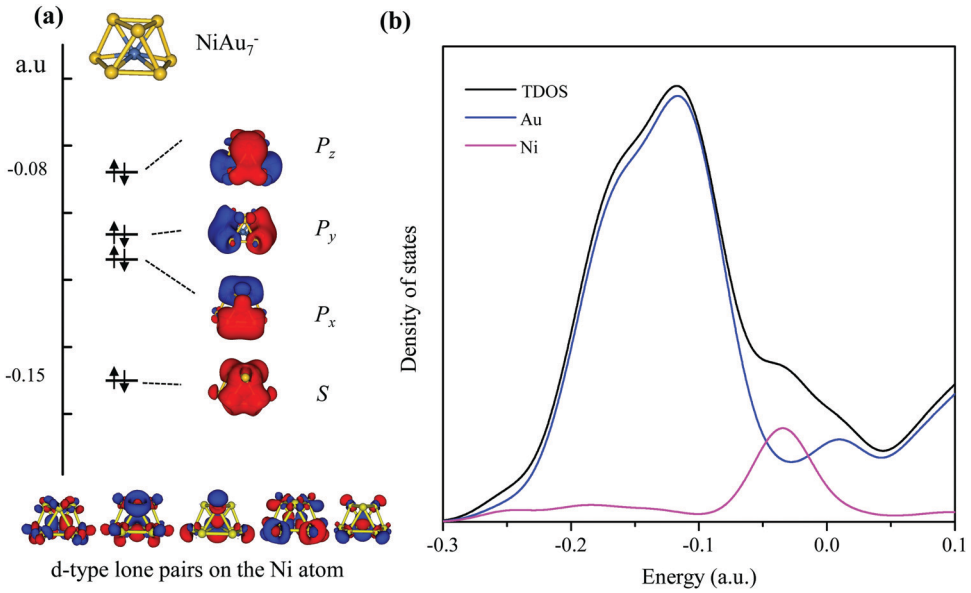

Fig. 2 (a) The molecular orbitals (MOs) and (b) density of states of the $NiAu_7^-$ cluster. The isosurface value is 0.02.

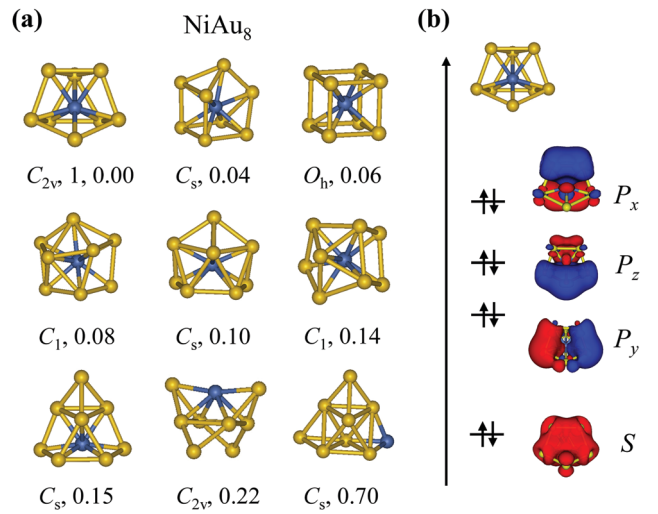

Fig. 3 (a) Optimized geometries of the low-energy isomers and (b) the MOs of $NiAu_8$ cluster at the TPSS/Def2-TZVP level. Labeled are symmetry, energy (eV) relative to the GM one and spin multiplicities. The isosurface value is 0.02.

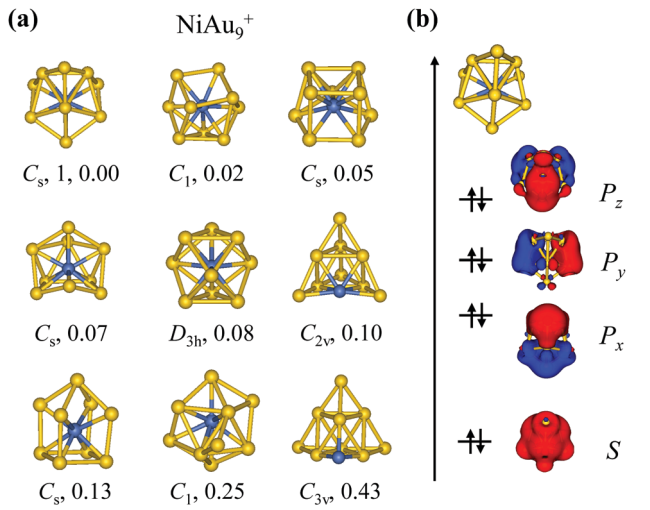

Fig. 4 (a) Optimized geometries of the low-energy isomers and (b) the MOs of the $NiAu_9^+$ cluster at the TPSS/Def2-TZVP level. Labeled are symmetry, energy (eV) relative to the GM one and spin multiplicities. The isosurface value is 0.02.

was determined. As shown in Fig. 3b, eight valence electrons of Au atoms occupy four superatomic orbitals ($1S^21P^6$) respectively. So the $NiAu_8$ cluster also satisfies the jellium model and can be regarded as a stable 18e superatom. Compared with the $NiAu_7^-$, the three P-type superatomic orbitals are different in the order of energy levels.

Fig. 4a shows the isomer shapes of the $NiAu_9^+$ cluster and their point group symmetry, and relative energies are arranged in order from low to high. The lowest energy of all the isomers of $NiAu_9^+$ is a spherical structure with C_s symmetry, in which the Ni atom is still highly coordinated. After the structure was precisely determined, we also calculated the molecular orbitals of the $NiAu_9^+$ cluster. As shown in Fig. 4b, the eight valence electrons of Au atoms occupy 4 superatomic orbitals ($1S^21P^6$) respectively. Therefore, the cation $NiAu_9^+$ also satisfies the jellium model and can be regarded as a stable 18e superatom. Overall, the transition metal Ni atom in the compact Au-based clusters presents one full-filling electron structure of d^{10}. In other words, the 10 valence electrons of the Ni atom are completely localized. When the valence electrons of Ni atoms do not contribute to the doped clusters, the geometric structures of the Au clusters can still be significantly changed. So this is an effective strategy for finding new types of metal superatoms.

The adiabatic ionization potentials, adiabatic electron affinities and HOMO–LUMO gaps of these three clusters are listed in Table S2 (ESI†), respectively. We note that $NiAu_9^+$ and $NiAu_8$ have relatively large ionization potentials, while $NiAu_7^-$ and $NiAu_8$ have relatively lower electron affinities. In particular, the small HOMO–LUMO gaps of the alloy clusters indicate that they may possess activation potentials. Moreover, the geometric structures of other neighboring sizes [$NiAu_n$ (n = 6–10)] are also observed, and their isomers are shown in Fig. S2 (ESI†). It is found that the structures of pure Au clusters are significantly altered by an additionally doped Ni atom.

3.2 Adsorption properties of Ni atom doped Au clusters

The research of gold-based alloy nanostructures to catalyze CO molecules has attracted more and more attention not only because of their influences on environmental processes, but also because of their simple adsorption behaviors.[40,41] However, there are plenty of possible sites for adsorption of CO molecules on the surface of one cluster. So it is indispensable that several basic rules for quickly finding these sites are summarized. In general, metal clusters consisting of two kinds of difference metal atoms result in an uneven distribution of charge over all surfaces of the clusters. Calculating the molecular electrostatic potential $V(r)$ is a well-developed method for analyzing inter-molecular interactions, charge distributions on the surfaces of the clusters and chemical bonding very intuitively.[51] In comparison with other charge distribution descriptors, the $V(r)$ method is an intuitively physical observable that is calculated from a theoretical and experimental electron density distribution. The value of the $V(r)$ of one atom is positive everywhere due to the fact that it is spherically symmetrical, while the value will be monotonically decreasing toward zero when leaving away from its nucleus. Finally, the formation of metal clusters will cause rearrangements of their electron densities toward more electronegative metal atoms and generate the corresponding negative regions. Therefore, the computation of the surface electrostatic potentials is very effective for quickly determining the adsorption sites of molecules on metal clusters. In other words, the $V(r)$ surfaces have been shown to be useful to characterize catalytic sites on metallic clusters, and detailed information of the intrinsic local reactivity at different sites can be obtained.

Fig. 5 plots the electrostatic potential $V(r)$ surfaces of the $NiAu_7^-$, $NiAu_8$ and $NiAu_9^+$ clusters, in which these alloy superatoms have geometrical and electronic shell closure structures. The positive regions of $V(r)$ surfaces are indicated in blue, and the negative regions are shown in red. Among them, the surfaces of $NiAu_7^-$ and $NiAu_9^+$ clusters distributed negative and positive charges, respectively. In comparison, the $NiAu_8$ cluster possesses remarkable σ-hole sites with positive potential regions where they are regions of depleted electron density. The σ-hole sites are the favored positions for electrostatically driven interactions with electron donating molecules. Hence, already from this analysis, there are indications that such site with σ-hole can be directly correlated with interaction strengths for one CO molecule that is a Lewis base. These also

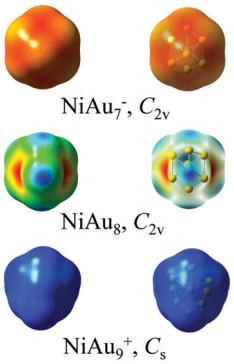

Fig. 5 Electrostatic potential surfaces of $NiAu_7^-$, $NiAu_8$ and $NiAu_9^+$ clusters. Positive surfaces (σ-holes) are depicted in blue, and negative in red.

indirectly indicate that the reactivity of different interaction sites of the systems is sensitive to chemical elements on cluster surfaces exhibiting a local reactivity.

The optimized isomers of the closed-shell $NiAu_8$ with CO molecule are illustrated in Fig. 6, and the vibration frequencies are calculated to check that they are real local minima on the potential energy surfaces. We considered more adsorption sites to evaluate the effectiveness of using σ-hole to determine the optimal adsorption sites, involving top sites, the hollow and bridge sites. Many adsorption structures have imaginary frequencies, or can't converge to stable structures. Among these isomers, the σ-hole adsorption structures are quickly identified as belong to true local minimums. Here, it shall be pointed out that, although there are perhaps existences of other local minima, we are focused on an important minimum wherein a Lewis bases molecule can approach one significant σ-hole site in the $V(r)$ surfaces of the $NiAu_8$. Dissecting the interactions in more detail, the Lewis base, CO molecules, interact preferentially with the most positive regions of $V(r)$ surfaces of the cluster, because one lone pair electrons localized on the C atom can be regarded as the active electron donor. In fact, it has previously been shown that the values of the $V(r)$ on the C atom of CO are more negative than that of the O atom. Therefore, the C head of the CO molecule binds to electron-deficient regions more easily than the O head. The MO diagrams of the adsorbed structure are also given in Fig. S3 (ESI†), in which the HOMO−1

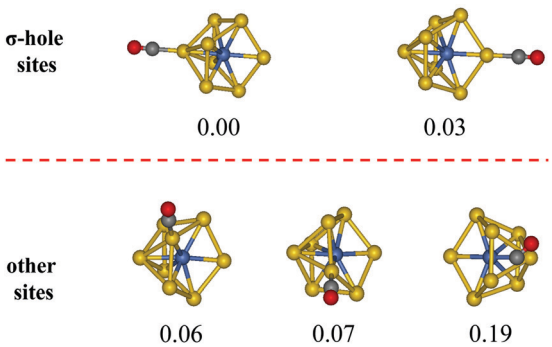

Fig. 6 The optimized isomers of the $NiAu_8$–CO structure. Labeled is the energy (eV) relative to the σ-hole adsorption structure.

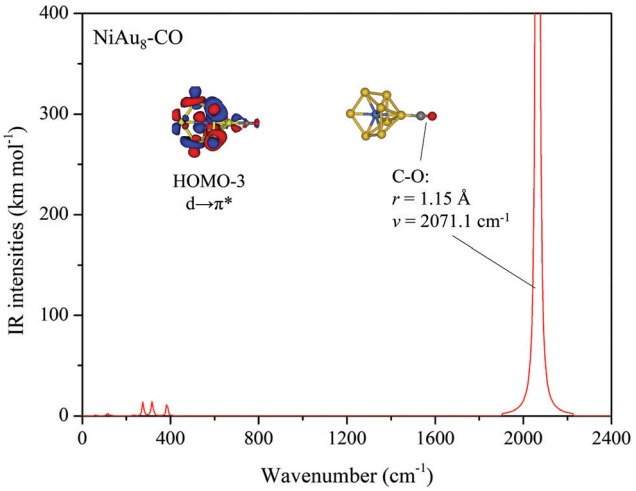

Fig. 7 The structure and infrared spectra (IR) of the $NiAu_8$–CO cluster.

and HOMO−3 orbitals illustrate the donor–acceptor interactions between the alloy superatom and the CO molecule. The results show that the σ-hole site indeed can cause a significant red-shift of the C–O bond.

We calculated the infrared spectra (IR) of the $NiAu_8$–CO structure, and the result is shown in Fig. 7. The C═O bond distance is 1.15 Å, which is slightly elongated than that of free CO molecules (1.128 Å). This is because that 5d electrons of the Au atom of the alloy superatom transfer towards the anti-bond π orbital of the CO molecule, as shown in the HOMO−3 orbital of the $NiAu_8$–CO. Furthermore, we find that the interaction energy between CO and the superatom is 1.21 eV, and the major interaction is the σ-donation coordination from the 5σ orbital of the CO molecule to the alloy cluster. The vibration frequency of the CO molecule (2071.1 cm^{-1}) is less than that of the free CO (2208 cm^{-1}),[59] which also further verifies transfers of 5d electrons in the superatom to the anti-bond π orbitals of the CO molecule. The result is in a significant red-shift for the C═O vibration frequency. The analysis shows that the classical metals bind the CO ligand *via* donor–acceptor interactions. Hence, the cluster may serve as one potential catalyst for the C–O covalent bond activation.

4. Conclusions

In summary, we investigated the effects of one Ni atom on the structures and properties of Au clusters. First, we searched the structures of $NiAu_7^-$, $NiAu_8$ and $NiAu_9^+$ clusters using the GA-DFT method, and found that these alloy clusters are all 3D spherical structures. The molecular orbitals and density of states analysis indicate that they have completely filled superatomic shells ($1S^21P^6$), in which the electronic structures of Ni atoms are all d^{10}. Electrostatic potential calculations show that the $NiAu_8$ superatom has remarkable σ-holes with positive potential regions, and these electron-deficient regions can be considered as interaction sites with some electron donors. When a Lewis base CO gas molecule is adsorbed on the Au-based superatom, we found that the C–O bond distance becomes slightly elongated and its stretching frequency presents a significant red-shift. This is due to the fact that 5d electrons of the Au atom of the $NiAu_8$ superatom transfer towards the anti-bond π orbital of the CO molecule. Hence, this is an effective strategy for finding new types of superatoms and potential catalysts for the covalent bond activation.

Conflicts of interest

There are no conflicts to declare.

Acknowledgements

This work is financed by the National Natural Science Foundation of China (21873001) and the Key Project of Scientific Research Foundation of Anhui Province Education Department (KJ2020A0646). The calculations were carried out at the High-Performance Computing Center of Anhui University.

References

1 H. Häkkinen, *Chem. Soc. Rev.*, 2008, **37**, 1847–1859.
2 M. Chen and D. Goodman, *Science*, 2004, **306**, 252–255.
3 Z. Li, H.-Y. T. Chen, K. Schouteden, T. Picot, T.-W. Liao, A. Seliverstov, C. Van Haesendonck, G. Pacchioni, E. Janssens and P. Lievens, *Sci. Adv.*, 2020, **6**, 4289.
4 G. Li and R. Jin, *Acc. Chem. Res.*, 2013, **46**, 1749–1758.
5 A. E. Green, S. Schaller, G. Meizyte, B. J. Rhodes, S. P. Kealy, A. S. Gentleman, W. Schöllkopf, A. Fielicke and S. R. Mackenzie, *J. Phys. Chem. A*, 2020, **124**, 5389–5401.
6 Y. Gao, S. Bulusu and X. C. Zeng, *J. Am. Chem. Soc.*, 2005, **127**, 15680–15681.
7 I. Dolamic, B. Varnholt and T. Bürgi, *Nat. Commun.*, 2015, **6**, 1–6.
8 M. Zhu, H. Qian, X. Meng, S. Jin, Z. Wu and R. Jin, *Nano Lett.*, 2011, **11**, 3963–3969.
9 P. Pyykko, *Chem. Rev.*, 1988, **88**, 563–594.
10 S. Pande, W. Huang, N. Shao, L.-M. Wang, N. Khetrapal, W.-N. Mei, T. Jian, L.-S. Wang and X. C. Zeng, *ACS Nano*, 2016, **10**, 10013–10022.
11 R. M. Olson, S. Varganov, M. S. Gordon, H. Metiu, S. Chretien, P. Piecuch, K. Kowalski, S. A. Kucharski and M. Musial, *J. Am. Chem. Soc.*, 2005, **127**, 1049–1052.
12 P. V. Nhat, N. T. Si and M. T. Nguyen, *J. Phys. Chem. A*, 2020, **124**, 1289–1299.
13 N. Shao, W. Huang, W.-N. Mei, L. S. Wang, Q. Wu and X. C. Zeng, *J. Phys. Chem. C*, 2014, **118**, 6887–6892.
14 A. Muñoz-Castro, *ChemPhysChem*, 2016, **17**, 3204–3208.
15 H. Schmidbaur and A. Schier, *Chem. Soc. Rev.*, 2012, **41**, 370–412.
16 L. Ferrighi, B. Hammer and G. K. Madsen, *J. Am. Chem. Soc.*, 2009, **131**, 10605–10609.
17 W. Huang and L.-S. Wang, *Phys. Rev. Lett.*, 2009, **102**, 153401.

18 J. Li, X. Li, H.-J. Zhai and L.-S. Wang, *Science*, 2003, **299**, 864–867.
19 M. P. Johansson, D. Sundholm and J. Vaara, *Angew. Chem., Int. Ed.*, 2004, **116**, 2732–2735.
20 F. Furche, R. Ahlrichs, P. Weis, C. Jacob, S. Gilb, T. Bierweiler and M. M. Kappes, *J. Chem. Phys.*, 2002, **117**, 6982–6990.
21 S. Gilb, P. Weis, F. Furche, R. Ahlrichs and M. M. Kappes, *J. Chem. Phys.*, 2002, **116**, 4094–4101.
22 A. Shayeghi, R. L. Johnston, D. M. Rayner, R. Schäfer and A. Fielicke, *Angew. Chem., Int. Ed.*, 2015, **54**, 10675–10680.
23 P. Ferrari, J. Vanbuel, E. Janssens and P. Lievens, *Acc. Chem. Res.*, 2018, **51**, 3174–3182.
24 S. Neukermans, E. Janssens, H. Tanaka, R. Silverans and P. Lievens, *Phys. Rev. Lett.*, 2003, **90**, 033401.
25 H. Tanaka, S. Neukermans, E. Janssens, R. E. Silverans and P. Lievens, *J. Chem. Phys.*, 2003, **119**, 7115–7123.
26 P. Pyykkö and N. Runeberg, *Angew. Chem., Int. Ed.*, 2002, **41**, 2174–2176.
27 Q. Du, X. Wu, P. Wang, D. Wu, L. Sai, R. B. King, S. J. Park and J. Zhao, *J. Phys. Chem. C*, 2020, **124**, 7449–7457.
28 W. Knight, K. Clemenger, W. A. de Heer, W. A. Saunders, M. Chou and M. L. Cohen, *Phys. Rev. Lett.*, 1984, **52**, 2141.
29 S. Khanna and P. Jena, *Phys. Rev. Lett.*, 1992, **69**, 1664.
30 Q. Liu and L. Cheng, *J. Alloys Compd.*, 2019, **771**, 762–768.
31 Q. Liu, C. Xu, X. Wu and L. Cheng, *Nanoscale*, 2019, **11**, 13227–13232.
32 X. Zhang, Y. Wang, H. Wang, A. Lim, G. Gantefoer, K. H. Bowen, J. U. Reveles and S. N. Khanna, *J. Am. Chem. Soc.*, 2013, **135**, 4856–4861.
33 Z. Luo and A. W. Castleman, *Acc. Chem. Res.*, 2014, **47**, 2931–2940.
34 D. E. Bergeron, A. W. Castleman, T. Morisato and S. N. Khanna, *Science*, 2004, **304**, 84–87.
35 Q. Wu, L. Zhou, G. C. Schatz, Y. Zhang and H. Guo, *J. Am. Chem. Soc.*, 2020, **142**, 13090–13101.
36 Q. Sun, P. Jena, Y. D. Kim, M. Fischer and G. Ganteför, *J. Chem. Phys.*, 2004, **120**, 6510–6515.
37 H. Xu, D. Cheng, Y. Gao and X. C. Zeng, *ACS Catal.*, 2018, **8**, 9702–9710.
38 S. Lin and Y. Pei, *J. Phys. Chem. C*, 2014, **118**, 20346–20356.
39 R. Pal, L.-M. Wang, Y. Pei, L.-S. Wang and X. C. Zeng, *J. Am. Chem. Soc.*, 2012, **134**, 9438–9445.
40 Y. Gao, N. Shao, Y. Pei and X. C. Zeng, *Nano Lett.*, 2010, **10**, 1055–1062.
41 W. T. Wallace and R. L. Whetten, *J. Am. Chem. Soc.*, 2002, **124**, 7499–7505.
42 H.-L. Chen, C.-H. Su and H.-T. Chen, *Chem. Phys. Lett.*, 2012, **536**, 100–103.
43 P. Rodríguez-Kessler, A. Muñoz-Castro, P. Alonso-Dávila, F. Aguilera-Granja and A. Rodríguez-Domínguez, *J. Alloys Compd.*, 2020, **845**, 155897.
44 A. C. Reber and S. N. Khanna, *Acc. Chem. Res.*, 2017, **50**, 255–263.
45 A. Walker, *J. Chem. Phys.*, 2005, **122**, 094310.
46 E. N. Esenturk, J. Fettinger and B. Eichhorn, *Chem. Commun.*, 2005, 247–249.
47 R. Ferrando, A. Fortunelli and R. L. Johnston, *Phys. Chem. Chem. Phys.*, 2008, **10**, 640–649.
48 W. Liu and L. Cheng, *J. Phys. Chem. C*, 2016, **120**, 2432–2438.
49 J. Tao, J. P. Perdew, V. N. Staroverov and G. E. Scuseria, *Phys. Rev. Lett.*, 2003, **91**, 146401.
50 L. Yan, L. Cheng and J. Yang, *J. Phys. Chem. C*, 2015, **119**, 23274–23278.
51 J. H. Stenlid and T. Brinck, *J. Am. Chem. Soc.*, 2017, **139**, 11012–11015.
52 M. Frisch, G. Trucks, H. Schlegel, G. Scuseria, M. Robb, J. Cheeseman, G. Scalmani, V. Barone, B. Mennucci and G. Petersson, Gaussian Inc., Wallingford, CT, 2010.
53 U. Varetto, Swiss National Supercomputing Centre, Manno, Switzerland, 2009.
54 F. Remacle and E. Kryachko, *J. Chem. Phys.*, 2005, **122**, 044304.
55 H. Häkkinen, M. Moseler and U. Landman, *Phys. Rev. Lett.*, 2002, **89**, 033401.
56 X. Wu and Y. Dong, *New J. Chem.*, 2014, **38**, 4893–4900.
57 H. Häkkinen, B. Yoon, U. Landman, X. Li, H.-J. Zhai and L.-S. Wang, *J. Phys. Chem. A*, 2003, **107**, 6168–6175.
58 D. Bandyopadhyay and P. Sen, *J. Phys. Chem. A*, 2010, **114**, 1835–1842.
59 X. Wu, L. Zhao, J. Jin, S. Pan, W. Li, X. Jin, G. Wang, M. Zhou and G. Frenking, *Science*, 2018, **361**, 912–916.

